DOI: https://doi.org/10.14256/JCE.2755.2019

Građevinar 9/2020

Primljen / Received: 25.10.2019.
Ispravljen / Corrected: 31.1.2020.
Prihvaćen / Accepted: 26.6.2020.
Dostupno online / Available online: 10.10.2020.

Effect of openings on cold formed steel shear wall panels

Authors:

Idriss Rouaz, PhD. CE
University of Blida,Algeria
Department of Civil Engineering
Geomaterials and Civil Engineering Laboratory
National Centre of Studies and Integrated Research on Building Engineering (CNERIB)
Rouaz.Idriss@gmail.com
Corresponding author

Prof. **Nouredine Bourahla**, PhD. CE
National School Polytechnic ENP, Algeria
Department of Civil Engineering
nedbourahla@gmail.com

Smail Kechidi, PhD. CE
University of Porto, Portugal
Faculty of Engineering
kechidi@fe.up.pt

Research Paper

Idriss Rouaz, Nouredine Bourahla, Smail Kechidi

Effect of openings on cold formed steel shear wall panels

In this paper, the effect of openings on global performance of Cold Formed Steel Shear Wall Panels is investigated numerically using the ABAQUS software. A benchmark model is first validated in terms of lateral shear capacity and nonlinear behaviour of the CFS-SWP. The failure mode of the CFS-SWP with opening is identified and validated. Subsequently, a parametric study on the effect of size and position of openings is conducted, in which the opening position is found to have a significant impact on the CFS-SWP performance. The benchmark model can be used for design purposes to evaluate with good accuracy the reduced ultimate strength of individual CFS-SWPs for any size and position of openings.

Key words:

cold formed steel shear wall panel, shear strength, nonlinear behaviour, connection failure, opening effect

Prethodno priopćenje

Idriss Rouaz, Nouredine Bourahla, Smail Kechidi

Utjecaj otvora na hladno oblikovane čelične posmične zidne panele

U radu se numeričkim postupkom istražuje utjecaj otvora na cjelokupno ponašanje hladno oblikovanih čeličnih posmičnih zidnih panela (CFS-SWP) s oblogom od rebrastog lima. Prvo je provedena validacija referentnog numeričkog modela u smislu posmične otpornosti i nelinearnog ponašanja CFS-SWP-a. Definiran je i provjeren način sloma CFS-SWP-a s otvorom. Zatim je provedena parametarska studija o utjecaju veličine i položaja otvora, te je utvrđeno da položaj otvora bitno utječe na učinkovitost CFS-SWP-a. Referentni se model može koristiti u fazi projektiranja za prilično točno ocjenjivanje umanjene krajnje otpornosti pojedinačnih CFS-SWP-a za bilo koju veličinu i položaj otvora.

Ključne riječi:

hladno oblikovani čelični posmični zidni panel, posmična otpornost, nelinearno ponašanje, slom spoja, utjecaj otvora

Vorherige Mitteilung

Idriss Rouaz, Nouredine Bourahla, Smail Kechidi

Einfluss von Öffnungen auf kaltgeformte Stahlschiebewandpaneele

Die Arbeit untersucht den Einfluss von Öffnungen auf das Gesamtverhalten von kaltgeformten Stahlschiebewandpaneelen (CFS-SWP). Zunächst wurde die Validierung hinsichtlich Scherfestigkeit und nichtlinearem Verhalten des CFS-SWP durchgeführt. Die Bruchart des CFS-SWP mit Öffnung wurde definiert und verifiziert. Anschließend wurde eine parametrische Untersuchung der Wirkung von Größe und Position der Öffnung durchgeführt, und es wurde festgestellt, dass die Position der Öffnung die Wirksamkeit von CFS-SWP wesentlich beeinflusst. Das Referenzmodell kann in der Planungsphase verwendet werden, um den verringerten Endwiderstand einzelner CFS-SWPs für jede Öffnungsgröße und -position ziemlich genau abzuschätzen.

Schlüsselwörter:

kaltgeformte Stahlschiebewandpaneel, Scherfestigkeit, nichtlineares Verhalten, Fugenversagen, Einfluss der Öffnung

1. Introduction

Cold formed steel (CFS) shear wall panels (SWP) sheathed with corrugated steel sheets have recently gained in popularity as they can resist severe lateral loads in highly seismic areas more effectively compared to others sheathing materials [1]. In addition, experimental research programs have been carried out [2-5] to evaluate the global behaviour and performance of CFS-SWP with this type of sheathing under lateral load.

However, for architectural and functionality design purposes, doors and/or windows openings need to be integrated into the SWP, which has an influence on its performance. The characterization of the lateral behaviour of the CFS-SWP is therefore considered necessary.

Fulop and Dubina [6] carried out an experiment with CFS-SWP to get a better insight of the global behaviour and assess the opening effect on the performance of the CFS-SWP under seismic load; they concluded that there is a dependency on the screw-sheathed connections' mode of failure. Other related experiments have also been conducted [7-11].

The AISI North American Standard for Cold-Formed Steel Framing - Lateral Design of 2007 (AISI S213-07) provides design parameters for steel-and wood-sheathing of CFS-SWP to be adopted by engineers. However, due to the diversity of architectural dimensions in light gauge steel construction, the tabulated values of design parameters do not cover the full range of CFS-SWP configurations. Hence, a numerical approach has become necessary and, using finite element (FE) models, it has proven to be a good alternative in predicting the behaviour and assessing the shear strength of the SWP for various geometric and mechanical characteristics. Several FE models have been developed and various modelling techniques have been presented. Bahrebar et al. [12] studied the shear strength of SWP sheathed with steel plate sheets, taking into account buckling failure modes, in addition to buckling of thin steel members [13, 14].

In fact, connection failure is a widespread phenomenon in the CFS-SWP. Kechidi et al. [15] developed hysteresis models that consider strength and stiffness degradation as well as the pinching effect observed in the steel- and wood-sheathed CFS-SWP. Rouaz et al. [16] presented a comparison between two numerical approaches for shear strength evaluation based on connection shear failure. According to Niari et al. [17], material nonlinearity should be integrated into the FE model, so as to improve its accuracy regarding screw connection which affects global behaviour of the CFS-SWP. Furthermore, Hosseinzadeh et al. [18] suggested that geometric nonlinearity should be introduced in numerical simulation of the CFS-SWP lateral behaviour, which may occur in light gauge steel structural components. Vigh et al. [19] and Kalali et al. [20] also presented a modelling technique of the CFS-SWP sheathed with corrugated steel on a short panel without opening.

As far as the opening effect on the global performance of SWP is concerned, Farzampour et al. [21] investigated, numerically, this aspect on corrugated plate shear walls with hot-rolled steel framing elements (beam and columns). Dai [22] studied the opening effect on CFS-SWP with cassette sheathing, where all members of the SWP were made of cold formed steel, but the cassette sheathing is not in common use in engineering practice. The same author [23] developed a numerical model of CFS-SWP to explore the influence of sheathing boards and fixing boundary conditions. The corrugated steel sheet was modelled with a plain element having two equivalent elastic moduli along the perpendicular and parallel directions of the corrugated steel sheet. In addition, the material nonlinearity, which is a crucial factor in global response, was not taken into account in the FE model [23]. In this paper, a detailed FE model, elaborated and validated using available experimental data, is used to investigate the opening effect on the shear strength of the CFS-SWP sheathed with corrugated steel sheets under lateral load. The nonlinear response and the corresponding ultimate displacement are also explored. The opening effect (door and window) is studied with regard to the change in position and size.

2. Selection of tested CFS-SWP

A thorough investigation of the effect of openings on the lateral behaviour of SWP would require a tremendous experimental program. In order to overcome these constraints, a detailed FE benchmark model was developed and validated against available experimental data for further sensitivity analyses. For this purpose, a tested corrugated steel-sheathed SWP performed by Fulop, and Dubina [6], with and without opening, was selected to validate the numerical model. As depicted in Figure 1, the selected specimen without opening, having 3600 mm in length and 2440 mm in height, is composed of two U154/1.5 tracks and nine C150/1.5 studs. The studs are attached to the top and the bottom tracks of each side with two pairs of SPEDEC SL4-F-4.8x16 (d = 4.8 mm) self-drilling, self-tapping screws. Built-up cross sections of double stud (toe-to-toe) are placed at the ends of the SWP.

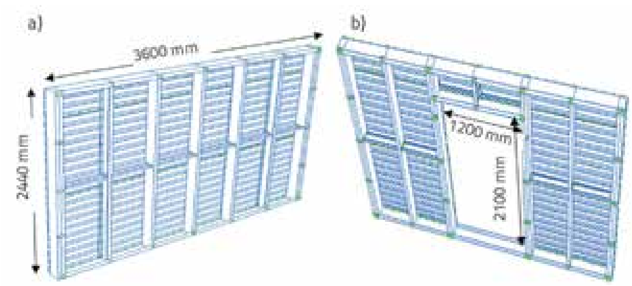

Figure 1. Selected tested SWP with corrugated-steel sheathing: a) SWP without opening; b) SWP with opening

As for intermediate studs (chord stud), single profile elements spaced at 600 mm intervals were adopted (Figure 2).

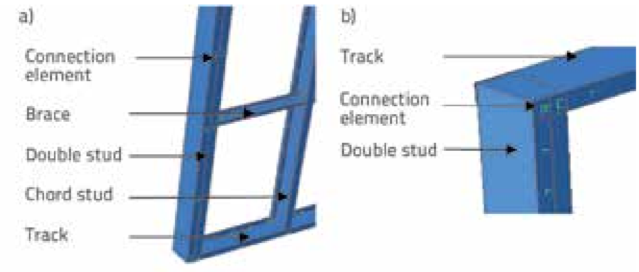

Figure 2. SWP details: a) Framing elements; b) chord-stud-to-track connection

Three corrugated steel sheets 1035 mm in width (Figure 3) are fixed on one side of the SWP frame with SD3-T15-4.8-22 self-tapping screws in each and every other corrugation in the intermediate studs. These steel sheets are placed in a horizontal position, where one overlapping corrugation is tightened with seam fasteners SL2-T-A14-4.8 × 20 at 200 mm intervals.

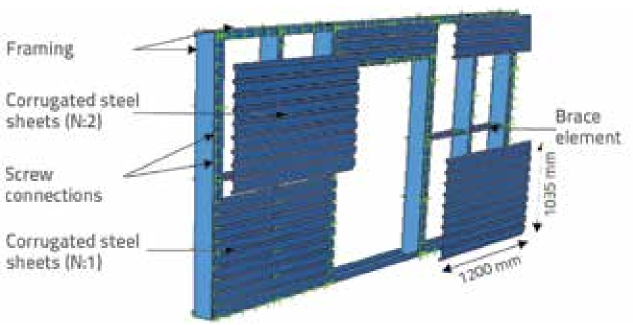

Figure 3. Corrugated steel sheathing assembled to the framing members

Table 1. Main geometrical characteristics

	Stud	Track	Brace	Sheathing
Dimension profiles	150 mm; 18 mm; 18 mm; 42 mm	154 mm; 55 mm	100 mm; 10 mm; 10 mm; 30 mm	12,5 mm; 12,5 mm; 65 mm; 12,5 mm; 18,5 mm
Thickness	1.5 mm			0.5 mm

In addition, horizontal brace members are installed at mid-height of the SWP to reduce twisting and buckling deformations of the stud. Six and four bracing members are placed in the SWP without and with opening, respectively. Table 1 shows main geometrical characteristics of the components of the selected SWPs. An additional chord stud is placed at each end of the opening for the corrugated-steel sheathed SWP, having 1200 x 2100 mm door opening (width x height).

3. Mechanical characteristics

3.1. Material properties

in order to characterize basic properties of materials used in SWP tests, mechanical properties of steel members similar to those of the selected panels were adopted from a normalized stress-strain curve in accordance with ASTM A635 G50 (Figure 4) [25].

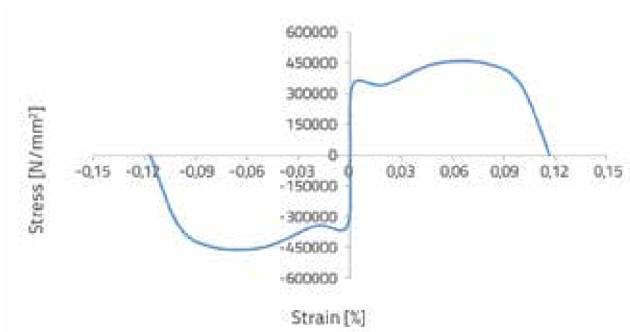

Figure 4. Stress-strain curve

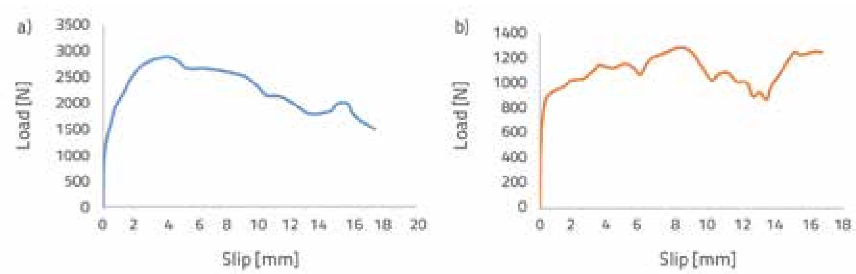

Figure 5. Load–displacement behaviour of screw connections [6]: a) joint of the lining with the frame; b) the joint of the lining with the lining

The yield stress f_y is 344 MPa, the tensile stress f_u is 448 MPa and the elastic modulus E_s is assumed to be $2.1 \cdot 10^5$ MPa. However, grade 70 steel (f_y = 483 MPa *and* f_u = 550 MPa) was used for corrugated steel sheets [26].

3.2. Screw connections

In order to take into account non-linearity behaviour of screw connections, which governs the global response and failure mode of the corrugated steel sheathed SWP, sheathing-to-sheathing and sheathing-to-framing screw connections were tested by Dubina [24]; Figure 5 shows the corresponding load-displacement curves.

Due to the lack of experimental data related to force–displacement curves of framing connections (stud and track), several series of experiments were undertaken by the author at the CNERIB laboratory, with the same conditions of thickness of members, tensile grade of steel framing, and screw diameter [24].

The screw test was carried out according to European Standards ECCS TC7 TWG 7.10 [27], and dimensions of test specimens (Figure 6) were selected as recommended in clause 3.2. The minimum number of tests was in compliance with clause 3.1.5 of the ECCS for the single fastener test.

As shown in Figure 7, test specimens were placed in the tensile test machine to determine the shear strength capacity and non-linear behaviour of one connection screw under monotonic load.

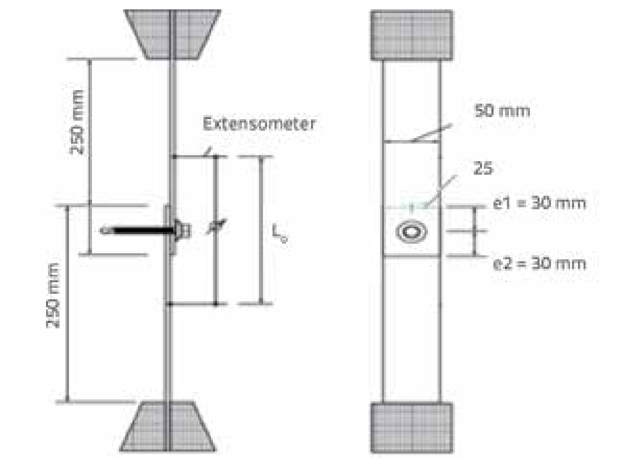

Figure 6. Dimension of test specimens


Figure 7. Specimen under tension test

As reported by Dubina and Fulop [24], the screw tilting and pullout was the dominant failure mode of the sheathing-to-sheathing and sheathing-to-framing screw fastener specimens, whereas the failure mode in framing-to-framing connections was dominated by shear of screw fasteners. Figure 8 shows the load–displacement result of the three tested assemblies.

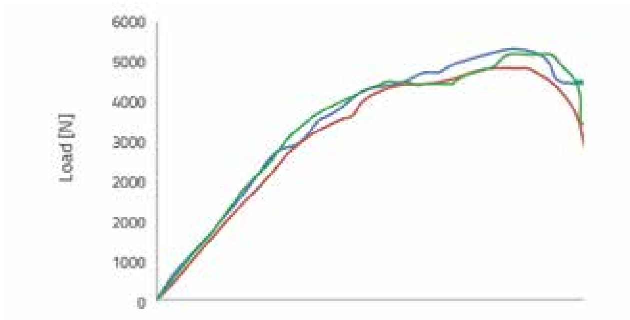

Figure 8. Framing-to-framing screw connection test result

4. Finite element modelling

SWPs are complex assemblies made of CFS members attached to sheathing using screw-fastened connections. When modelling this subsystem, particular attention is required with regard to the study of its overall behaviour and performance, taking into account main failure modes such as failure of screw-fastened connections, and the local or global buckling limit states of framing members. A detailed description of the FE modelling protocol of the selected SWPs is presented in this section using the commercial ABAQUS software [28].

4.1. Element types and meshing

Due to the large strain in SWP elements under horizontal monotonic load, it was deemed important to take into account geometric nonlinearity in the analysis. Hence, all elements, including sheathing, track, stud, and lateral channel bracings, were modelled as S4R shell elements with reduced integration scheme. Each element's node had three translational and three rotational degrees of freedom, which could be restrained according to experimental conditions.

Based on similar previous CFS-SWP studies conducted by Dai [22, 23] and Rouaz [16], in which sensitivity analysis was performed on mesh size elements, a good compromise in terms of time and accuracy was achieved with a mesh dimension close to 50 mm x 50 mm for all framing members. For the corrugated sheets, each unfastened side was divided into two parts in the horizontal direction, and 40 mm in the vertical direction was adopted as shown in Figure 9.

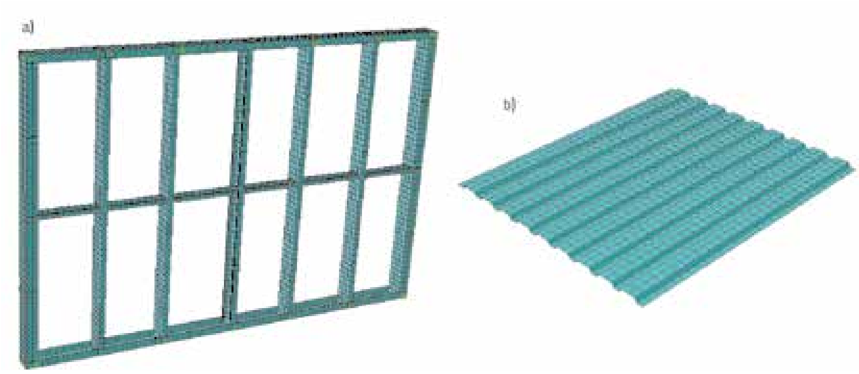

Figure 9. Model meshing of CFS-SWP: a) Framing; b) Sheathing

The surface-to-surface contact was used to model interaction between element members, namely, contact between track and stud flanges, and sheathing-to-framing contact. Based on sensitivity analysis performed by Dai [23], the results are not greatly affected by friction coefficient. Therefore, a friction factor of 0.3 was adopted in this study.

4.2. Mechanical properties of element members

In order to introduce material nonlinearities in the FE model, the engineering stresses (σ) and engineering strains (ε) obtained from normalized curves were converted to obtain the so-called true stress (σ_{tru}) and true strain (ε_{tru}) using the following equations [17]:

$$\sigma_{tru} = \sigma_{nom}\left(1+\varepsilon_{nom}\right) \quad (1)$$

$$\varepsilon_{tru} = \ln\left(1+\varepsilon_{nom}\right) \quad (2)$$

$$\varepsilon_{pl} = \varepsilon_{tru} - \frac{\sigma_{tru}}{E} \quad (3)$$

4.3. Structural properties of screw fastener elements

4.3.1. Tensile strength

The pull-out strength of the sheathing and framing screw connection is estimated using design provisions of the North American Specification for the Design of Cold-Formed Steel Structural Members AISI S100 (section E.4.4.1) [29]. The strength can be obtained using Eq. 4:

$$P_{not} = 0{,}85\left(t_c \cdot d\right)F_{u2} \quad (4)$$

where d is the nominal screw diameter, t_c is the lesser of the depth of penetration and thickness, P_{not} is the nominal pull-out strength per screw, and F_{u2} is the tensile strength of a member not in contact with the screw head or washer.

4.3.2. Shear mechanical characteristics

The nonlinear shear behaviour of screw fastener is considered as an envelope force-displacement response curve, as shown in Figure 10.

To simulate the damage evolution from point I, which represents the ultimate force, to point D, corresponding to ultimate displacement, each component is defined with ($\bar{u}_f^{pi}$, F_i) coordinates, where F_i is the damaging force, calculated as given in ABAQUS Manual [28]:

$$f_i = (1 - d_i)\, F_{effi} \quad (5)$$

F_{effi} is the effective force representing the ultimate force, and d_i is the damage variable given by equation (6) :

$$d_i = \frac{1-e^{-\alpha\frac{\bar{u}_u^{pl}-\bar{u}_0^{pl}}{\bar{u}_f^{pl}-\bar{u}_0^{pl}}}}{1-e^{-\alpha}} \quad (6)$$

where:

$\bar{u}_f^{pl}$ - equivalent plastic displacement damage at i component

$\bar{u}_0^{pl}$ - equivalent plastic displacement at damage initiation

α - exponential coefficient based on calibration with the experimental data curve

$\bar{u}_1^{pl}$ - equivalent plastic displacement at damage failure.

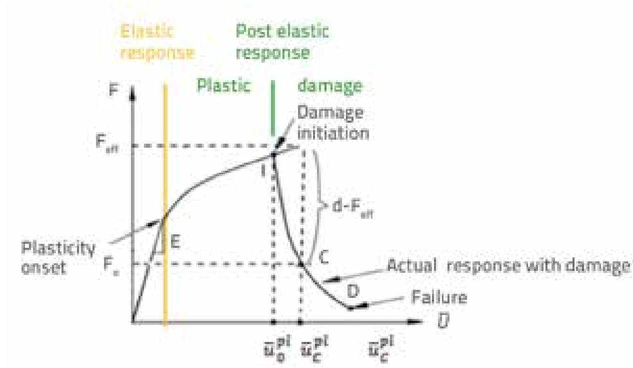

Figure 10. Connection behaviour modelling [28]

4.4. Connection modelling

In order to set a connection between two or more elements, ABAQUS has a comprehensive set of connection defining elements such as spot welds, rivets, screws, bolts and other types of mechanical fasteners. Furthermore, as shown in Figure 11, the fixing elements can be located anywhere regardless of the mesh nodes, which are known as "mesh-independent fasteners". Physical characteristics of the connector are then introduced into the "interaction" module and are defined as screws elements taking into account the spacing, diameter, orientation and influence of the radius of screws.

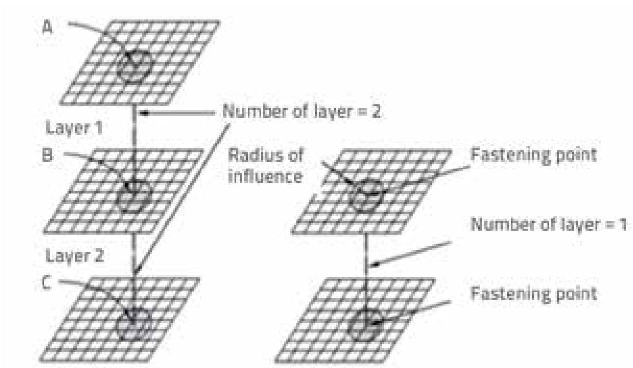

Figure 11. Mesh-independent fasteners [28]

4.5. Boundary condition and analysis

Two Tie Multi Point Control "MPC" interactions were used to simulate experimental boundary conditions of the SWP test set-up using the FE models. One was used to fasten the pinned bottom track to the ground in order to model the seven bolts placed in the vicinity of each stud, and the other was adopted to allow the application of displacement at the top track. The test rig that prevents any torsional movement of the wall or out-of-plane translation was modelled by restraints of translations in the out of plane direction.

Quasi-static nonlinear analyses were performed, with the initial increment size equal to 0.1 and the minimum increment size limited to $10 \cdot e^{-8}$. The full Newton–Raphson iteration method was used to solve nonlinear equations in the analysis.

5. Validation of numerical models

5.1. Shear strength-lateral displacement assessment

A comparison between numerical and experimental results was made for the selected SWP with and without opening in order to validate the above-described modelling protocol. Figure 12 shows the nonlinear curve of the shear strength-lateral displacement response under monotonic load.

As shown in Table 2, the ultimate shear strength (F) and the corresponding lateral displacement (U) are close to the corresponding experimental results, and the difference in shear strength (ΔF) is relatively low (2.40 % and 5.46 %) for SWPs with and without opening, respectively.

However, the difference in the initial stiffness and ultimate displacement is more pronounced in the case of the SWP with opening. This is mainly due to some simplistic modelling assumptions which do not take into account some properties such as the real mechanical material properties of the seven bolts installed in the bottom track of the specimen to fix the panel to the ground.

Table 2. Comparison between numerical and experimental results

	F [N]	U [mm]	K_0 [N/mm]	ΔF [%]	Δu [%]	ΔK_0 [%]
Without opening						
Experimental	52876.4	43.80	4500.50	/	/	/
Finite element	51610	40.03	3970.32	2.40	8.68	11.79
With opening						
Experimental	40220.2	62.69	1643.20	/	/	/
Finite element	38090	55	1423.60	5.46	12.27	13.36

Introducing the door opening in the SWP led to a decrease of about 24 % and 26 % of the shear strength obtained from experimental and numerical models, respectively, and to a 43 % increase in lateral displacement.

The error in predicting the ultimate shear strength and the corresponding lateral displacement is 2.5 % and 5.43 %, respectively. Therefore, this model will be used to investigate the effect of the opening on the shear strength of the SWP.

5.2. Failure mode assessment

Figure 13 shows the location of material failure of the corrugated steel sheets in order to confirm that the tensile stress developed in the sheathing is absorbed by sheathing-to-framing connections. This failure (highlighted in red) is initiated

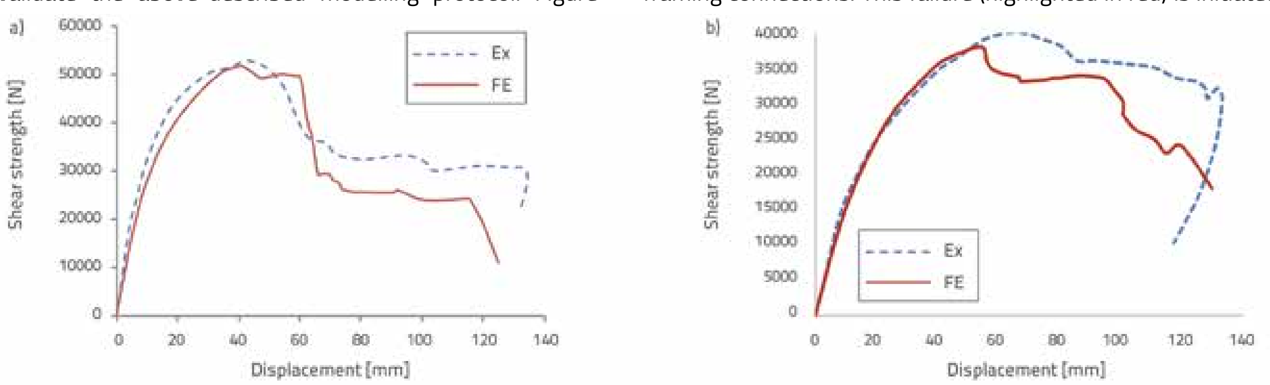

Figure 12. Comparison of numerical (FE) and experimental (Ex) test results: a) Without opening; b) With opening

at the corner of the SWP and the chord stud having tight screw spacing. The occurrence of failure at these locations means that the tensile stress was absorbed by these connections. On the other hand, framing-to-framing screw-fastened connections did not exhibit any damage over the entire loading range. It is worth noting that this trend has been observed in most of the previous experimental studies on CFS-SWPs.

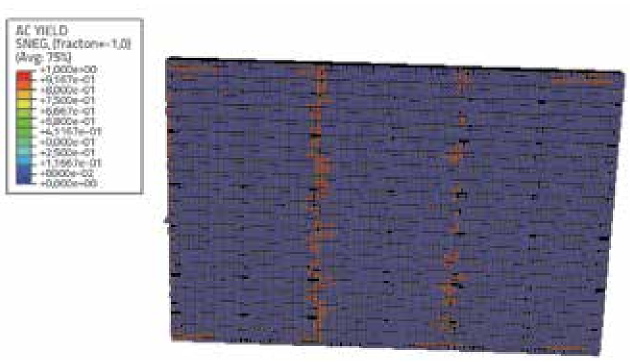

Figure 13. Failure connections localization of SWP without opening

Failure mode characteristics of the SWP with opening predicted by numerical simulation are illustrated in Figure 14.b. An important local buckling of the corrugated sheathing is clearly absorbed in the lintel region. In addition, a stress concentration appeared around the opening (1) and an uplift of the SWP corners can also be noted (2). Moreover, the failure of screw-fastened connections (3 and 4) occurred at two of the lower seams. Similar features characterized the failure mode of the test specimen.

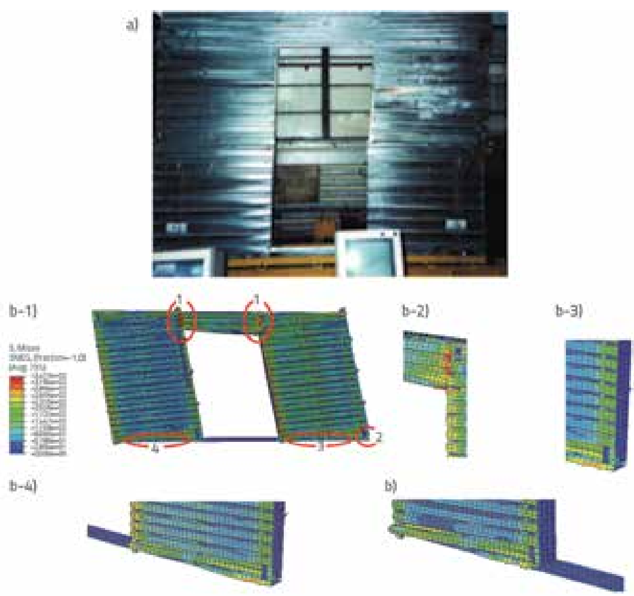

Figure 14. Failure modes of SWP with opening: a) Experimental results; b) FE simulations (b-1) Entire SWB, (b-2) Stress concentration around the opening (1), (b-3) Uplift of SWP corners (2), (b-4) Failure of screw fastener connections occurred at the bottom of the SWP (3, 4)

6. Parametric study

A parametric study was carried out using the above-described modelling protocol in order to evaluate the effect of the opening position and its area ratio on the shear strength of the SWP. Following architectural practice, the dimensions of door and window openings are 1200 mm x 2100 mm and 1200 mm x 800 mm, respectively. Typical positions of these openings are depicted in Figure 15 and, at that, the wall dimensions (3600 mm long and 2440 mm high) and the cross-section properties of the framing members were kept similar to those described in Section 2.

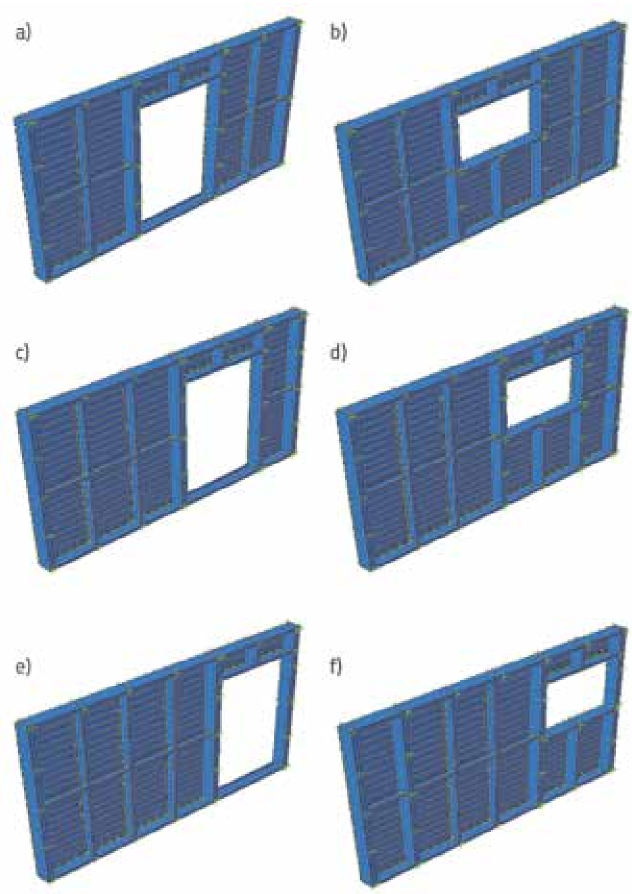

Figure 15. Positions of openings: a) Door opening (position-1); b) Window opening (position-1); c) Door opening (position-2); d) Window opening (position-2); e) Door opening (position-3); f) Window opening (position-3)

The shear strength-lateral displacement curves for the two areas ratios in three different positions are presented in Figure 16.

6.1. Effect of opening position

A comparison of the shear strength and the corresponding lateral displacement between the three locations of door and

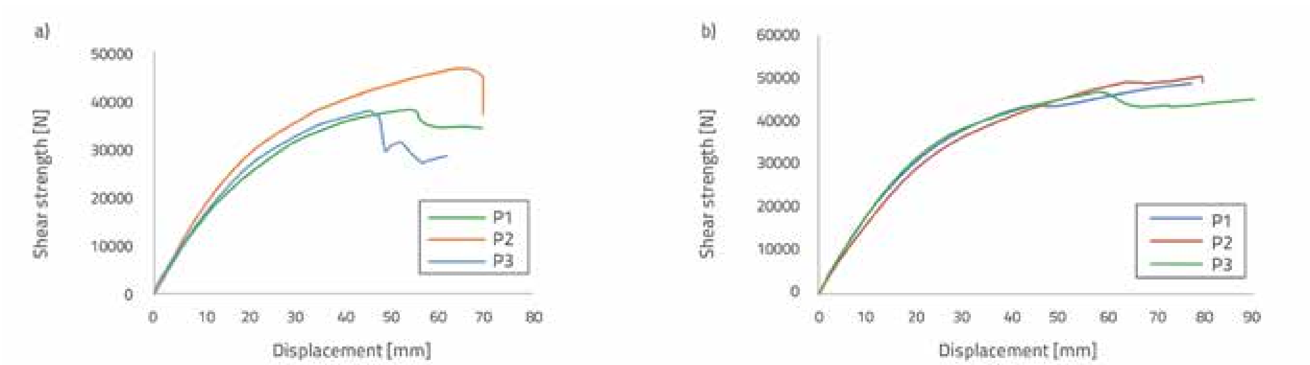

Figure 16. Response of the SWP with different areas and positions: a) Door opening; b) Window opening

window openings under monotonic load is made in this section. The central opening (position 1 in Figure 15) in the SWP is taken as a benchmark.

6.1.1. Door opening

The results listed in Table 3 show that the SWP with an opening located in position 2 exhibits a higher ultimate shear strength and a large lateral displacement. In fact, two rows of screw connections are installed on the intermediate stud to connect the ends of the corrugated sheets to the SWP framing. This position (2) has an additional row of screw connections compared to others positions (*i.e.*, 1). This configuration with additional screw connections, as compared also to position 3 (due to the lack of screw connections in the chord-stud in the vicinity of the opening), has resulted in an increased shear capacity of the SWP.
Moreover, regarding this number of screw connection rows, the SWP with an opening located in position 3 has one screw connection row less than the benchmark case (1), leading to a slightly lower ultimate shear capacity and a larger corresponding lateral displacement due to the reduced number of screw connections. Moreover, a significant distortion appeared at the end of chord stud (Figure 17.a) due to the narrow sheathing lintel at the top of the door.

Table 3. Comparison of opening door position effect

Position	Shear strength [N]	Displacement [mm]	Shear strength [%]	Displacement [%]
1	38090	55	-	-
2	45650	66	22.23	20.00
3	36577	45	-2.72	-17.55

6.1.2. Window opening

The window opening at different positions was also investigated in the same way as the door opening effect. Table 4 highlights an increase in ultimate shear strength and the corresponding lateral displacement in positions 2 and 3 as compared to the benchmark case. Furthermore, the best performance contribution of this window position is when the opening is between the centre and the end of the SWP (*i.e.*, position 2), which has a greater influence on the ultimate lateral displacement than the shear strength.

Table 4. Comparing window opening position effect

Position	Shear strength [N]	Displacement [mm]	Shear strength [%]	Displacement [%]
1	43765	45	-	-
2	49058	64	12.09	42.22
3	46302	57	5.80	28.57

Despite the small difference in the number of screw connections between position 1 and position 3 (higher in position 1), the shear strength and lateral displacement are higher in position 1 than in position 3. This is due to the fact that, for an opening in position 1, the continuity of the diagonal tension field is no longer ensured compared to position 3. Furthermore, it can be noted that the pull-out screw-fastened connections located in position 3 (Figure 17.b) dominate the main failure mode, due to distortion of the left chord stud of the SWP.

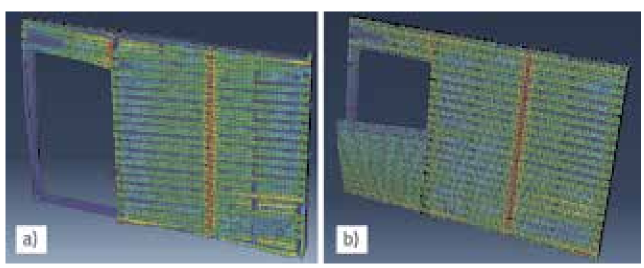

Figure 17. Failure modes of SWP with the opening located at its end (position 3): a) Door opening; b) Window opening

6.2. Effect of opening area in different positions

It was found that reducing the opening area by 2.6 times from door to window has not provided the same performance in the three positions. In terms of ultimate shear strength. Figure 18

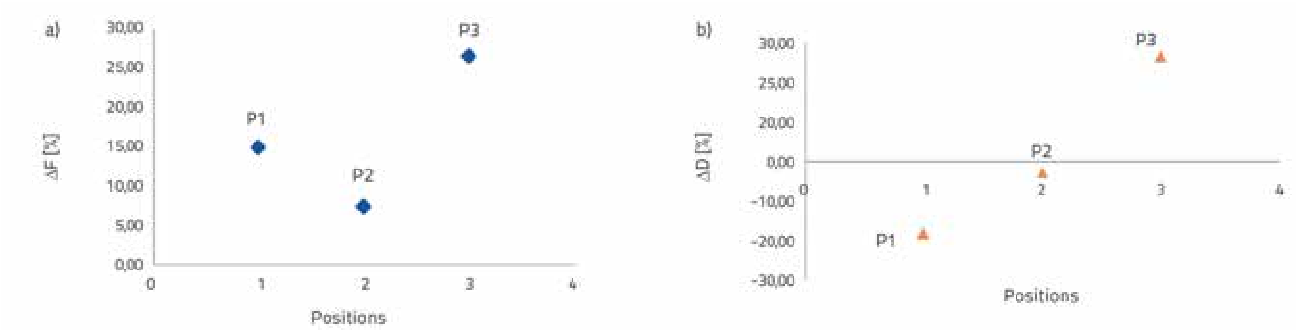

Figure 18. Opening area ratio effect in three positions: a) Shear strength; b) Ultimate displacement

shows that the other positions are more likely to provide better performance, particularly the third position, where an ultimate shear strength increased by up to 26.59 %. This is mainly due to the contribution of additional sheathing at the bottom corner of the SWP, which removes the opening installation of the diagonal tension.
Although the first position gives more capacity in terms of shear strength compared to the second position (2), a significant decrease of the ultimate displacement in this position (1) was obtained, which is unsuitable in engendering design. Moreover, the third position (3) has presented the large ultimate displacement of 26.26 %.

7. Conclusions

This paper presents the development and validation of a finite element (FE) modelling protocol for CFS-SWPs with and without openings, based on experimental results as well as a parametric study of the opening's effect on lateral behaviour of CFS-SWPs. It was found that:

- Taking into account the material, geometric and connection assembly nonlinearities, a good agreement has been reached between numerical and experimental results in terms of nonlinear behaviour, initial stiffness, ultimate shear strength, and the corresponding displacement.
- Discrepancies between numerical and experimental results for specimens with and without openings in terms of ultimate shear strength and displacement are of the order of 2.40 % and 5.46 % respectively. Therefore, the numerical modelling protocol developed for the SWP with opening is considered reliable for the purpose of parametric study.

According to this study, a special attention should be paid to the reducing effect of the opening area and its position on the shear capacity, such as:

- The door and window openings, located in the central position, have a tangible effect to decrease the shear capacity of the SWP by up to 26 % and 15 %, respectively, which must be considered by practicing engineers.
- The opening's position (door or window) between the central and the edge of the SWP produces better performance compared to other positions.
- The door opening in the central position has a smaller effect on the decrease in shear capacity of the SWP compared to the position at the edge of the SWP (position 3). However, in the case of the window opening, the opening's position at the edge of the SWP (position 3) has a lower effect on the decrease in shear strength than the central opening's position.
- Under monotonic load, it was shown that the door opening at the edge of the SWP induces an additional failure mode in the vicinity of the chord studs, and reduces more the ultimate displacement than the shear strength.

This study demonstrates the importance of numerical analysis in assessing the effect of openings on the shear strength of the SWPs, and can be a powerful tool to help the design engineer to evaluate with good accuracy the reduced strength capacity of individual CFS-SWPs with any size and position of openings.

REFERENCES

[1] Khaliq, W., Moghis, A.: Shear Capacity of Cold-Formed Light-Gauge Steel Framed Shear-Wall Panels with Fiber Cement Board Sheathing, International Journal of Steel Structures, 17 (2017) 4, pp 1404-1414.

[2] Emami, F., Mofid, M., Vafai, A.: Experimental study on cyclic behaviour of trapezoidally corrugated steel shear walls, Engineering Structures, 48 (2013), pp. 750–762, https://doi.org/10.1016/j.engstruct.2012.11.028.

[3] Yu, C., Yu, G.: Experimental Investigation of Cold-Formed Steel Framed Shear Wall Using Corrugated Steel Sheathing with Circular Holes, J. Struct. Eng, 142 (2016) 12, http://dx.doi.org/10.1061/(ASCE)ST.1943-541X.0001609.

[4] Yu, C.: Steel Sheet Sheathing Options for Cold-Formed Steel Framed Shear Wall Assemblies Providing Shear Resistance, Report No. UNT-G70752, American Iron and Steel Institute, Washington, DC. , 2009.

[5] Zhang, W., Mahdavian, M., Li, Y., Yu, C.: Experiments and Simulations of Cold-Formed Steel Wall Assemblies Using Corrugated Steel Sheathing Subjected to Shear and Gravity Loads, J. Struct. Eng, 4 (2016) 6, pp. 1-13. https://doi.org/0.1061/(ASCE)ST.1943-541X.0001681.

[6] Fulop, L.A., Dubina, D.: Performance of wall-stud cold-formed shear panels under monotonic and cyclic loading, Thin-Walled Structures, 26 (2004), pp. 321–338. https://doi.org/10.1016/S0263-8231(03)00063-6.

[7] Fiorino, L., Corte, D.G., Landolfo, R.: Experimental tests on typical screw connections for cold-formed steel housing, Engineering Structures, 29 (2007), pp. 1761–1773. https://doi.org/10.1016/j.engstruct.2006.09.006.

[8] DaBreo, J., Balh, N., Ong-Tone, C., Rogers, C.A.: Steel sheathed cold-formed steel framed shear walls subjected to lateral and gravity loading, Thin-Walled Structures, 74 (2014), pp. 232-2245, https://doi.org/10.1016/j.tws.2013.10.006.

[9] Peterman, K.D., Nakata, N., Schafer, B.W.: Hysteretic characterization of cold-formed steel stud-to-sheathing connections", Journal of Constructional Steel Research, 101 (2014) 5, pp. 254–264, https://doi.org/10.1016/j.jcsr.2014.05.019.

[10] Ding, C.: Monotonic and Cyclic Simulation of Screw-Fastened Connections for Cold- Formed Steel Framing, Master of Science in Civil Engineering. Dissertation, Virginia Polytechnic Institute, Virginia, 2015.

[11] Mohebbi, S., Mirghaderi R., Sabbagh, A.B., Farahbod, F.: Experimental work on single and double sided steel sheathed cold-formed steel shear walls for seismic actions", Thin-Walled Structures, 91 (2015), pp. 50–62, https://doi.org/10.1016/j.tws.2015.02.007.

[12] Bahrebar, M., Zaman, M., Kabir, M.H., Zirakian, T., James, B.P.: Structural Performance of Steel Plate Shear Walls with Trapezoidal Corrugations and Centrally-Placed Square Perforations", International Journal of Steel Structures, 16 (2016) 3, pp. 845-855, https://doi.org/10.1007/s13296-015-0116-y.

[13] Ghannam, M.: Axial Load Capacity of Cold-formed Steel Built-up Stub Columns", International Journal of Steel Structures, 17(2017) 4, pp. 1273-1283.

[14] Konkong, N., Aramraks, T., Phuvoravan, K.: Buckling Length Analysis for Compression Chord in Cold-Formed Steel Cantilever Truss, International Journal of Steel Structures, 17 (2017) 2, pp. 775-787.

[15] Kechidi, S., Bourahla, N.: Deteriorating hysteresis model for cold-formed steel shear wall panel based on its physical and mechanical characteristics, Thin-Walled Structures, 98 (2016), pp. 421–430, https://doi.org/10.1016/j.tws.2015.09.022.

[16] Rouaz, I., Bourahla, N.: Numerical evaluation of shear strength for Cold-Formed Steel Shear Wall Panel, International Journal of Civil, Environmental, Structural, Construction and Architectural Engineering, 10 (2016) 3, pp. 347–351, cholar.waset.org/1999.3/10004074.

[17] Niari, S.E., Rafezy, B., Abedi, K.: Seismic behaviour of steel-sheathed cold-formed steel shear wall: Experimental investigation and numerical modelling, Thin-Walled Structures, 96 (2015), pp. 337–347, https://doi.org/10.1016/j.tws.2015.08.024.

[18] Hosseinzadeh, S.A.A., Tehranizadeh, M.: Introduction of stiffened large rectangular openings in steel plate shear walls", Journal of Constructional Steel Research, 77 (2012), pp. 180–192, https://doi.org/10.1016/j.jcsr.2012.05.010.

[19] Vigh, L.G., Abbie, B.: Component model calibration for cyclic behaviour of a corrugated shear wall", Thin-Walled Structures, 75 (2014), pp. 53–62, https://doi.org/10.1016/j.tws.2013.10.011.

[20] Kalali, H., Ghazijahani, T.G., Hajsadeghi, M., Zirakian, T., Alaee, J.F.: Numerical Study on Steel Shear Walls with Sinusoidal Corrugated Plates, Latin American Journal of Solids and Structures, 13 (2016), pp. 2502-2514, https://doi.org/10.1590/1679-78252837.

[21] Farzampour, A., Jeffrey, A.: Behaviour prediction of corrugated steel plate shear walls with openings, Journal of Constructional Steel Research, 114 (2015), pp. 258-268, http://dx.doi.org/10.1016/j.jcsr.2015.07.018.

[22] Dai, X.: Structural Behaviour of Cold-formed Steel Cassette Wall Panels Subject to In-plane Shear Load, Journal of Civil Engineering Research, 3 (2013) 2, pp. 65–74. https://doi.org/10.5923/j.jce.20130302.01.

[23] Dai, X.: Numerical Modelling and Analysis of Structural Behaviour of Wall-stud Cold-formed Steel Shear Wall Panels under In-plane Monotonic Loads, Journal of Civil Engineering Research, 2 (2012) 5, pp. 31–41, https://doi.org/10.5923/j.jce.20120205.02.

[24] Dubina, D.: Behaviour and performance of cold-formed steel-framed houses under seismic action, Journal of Constructional Steel Research, 64 (2008), pp. 896–913. https://doi.org/10.1016/j.jcsr.2008.01.029.

[25] CSI, SAP2000. Computers and Structures, 2014.

[26] Fulop, L. A.: Contributions to the optimization of structural systems for one family houses with steel structures, Ph.D. Dissertation, Politehnica University of Timisoara, 2003.

[27] ECCS TC7 TWG 7.10. The testing of connections with mechanical fasteners in steel sheeting and sections, ECCS-European Convention for Constructional Steel-work. Portugal. 2009.

[28] Dassault Systems, Prescribed Conditions, Constraints, Interactions, Abaqus analysis user's manual, volume 5, USA. 2010.

[29] AISI, S100-2007, North American Specification for the Design of Cold-Formed Steel Members, American Iron and Steel Institute, Canada. 2007.